Advances in Science and Technology Research Journal

Advances in Science and Technology Research Journal, 2026, 20(3), 454–464
https://doi.org/10.12913/22998624/214673
ISSN 2299-8624, License CC-BY 4.0

Received: 2025.10.10
Accepted: 2025.11.29
Published: 2026.02.01

Analysis of electrical and thermal properties and the effect of thallium on energy emission from the cathode surface in arc plasma

Hasan Abedulhadi Kadhem[1*], Rafid Abbas Ali[1]

[1] Department of Physics, College of Science, Mustansiriyah University, Baghdad, Iraq
* Corresponding author's e-mail: hasanalsagad123456@gmail.com

ABSTRACT

The importance of this study lies in the use of a mercury-thallium for different levels of concentration and applied voltage mixture in arc plasma to enhance the efficiency of high-pressure lighting systems, reduce costs, and mitigate electrode corrosion. Mercury is the main element used in arc lamps. The addition of thallium has contributed to improving the emitted light characteristics and stability, reducing energy loss, and extending operating life. The NCPL model was used to interpret and analyze the physical changes in the region near the cathode surface. This model simulates the thermal and electrical interactions that control the transfer of current and energy density, providing accurate data that helps in optimizing high-pressure lighting systems, and measure the ratio of the ionization length to the mean free path, while the THERMCAT model was used to measure the total energy released from the cathode surface of a mixture of mercury and thallium at different concentration and applied voltage. At a concentration of (0.5 mol) of thallium in the mixture, it contributed to improving the physical and chemical properties due to the abundance of a large number of ionizable atoms. The energy flux increases along with cathode surface temperature, where the increase is linear at (<3500 K) and non-linear at (T_W > 3500 K). When the applied voltage is increased to (50 V), the energy flux (q) increases due to the acceleration of the charged particles in the electric field. This enhances their energy, leading to an increase in collisions between the charged particles. Whilst THERMCAT model The energy emitted from the cathode surface increases along with the diffusion or spot current, where the relationship is linear between the energy emitted from the cathode surface and the spot current due to the accumulation of charges and the rise in temperatures in the spot area.

Keywords: arc discharge, temperature of cathode surface, energy glow, ratio of the ionization length to the mean free path.

INTRODUCTION

Plasma is a state of matter composed of charged and neutral particles, characterized by its interaction with electric and magnetic fields. It occurs naturally in the ionosphere, the upper atmosphere, stars, as well as interstellar regions, and represents the largest proportion of visible matter in the universe [1,2]. Arc discharge has distinct characteristics in that the current density is very high while the potential difference is low, which causes high temperatures and consequently ionization of the mixture [3,4], Because arc discharge has thermal properties and ionization of gas or mixture molecules, it is used in various industrial applications, such as metal cutting, welding, and modern materials production technologies [5]. Arc discharge lamps are a type of advanced lighting system that is used to produce light by ionizing gas molecules through the passage of an electric current through the mixture. They are characterized by their high efficiency and long life without the need to heat the filament as in traditional lamps, which makes them a suitable choice for lighting large spaces [6,7]. This study aimed to determine the effect of adding thallium to the mercury gas mixture in discharge lamps and improving the energy transfer

processes, electron emission from the cathode surface, as well as changes in electrical and chemical properties. The importance of the study was to explain and analyze the mechanisms of the reactions that occur near the cathode surface. This study improved lighting stability, reduced energy consumption, and prolongs the life of lamps, as mercury has a low ionization potential, making it suitable for ultraviolet lamps, and has a long operating life [8].Yoon and his team developed a dual technology that combines low-voltage arc discharge and microwave plasma. This technology extends the system's life, reduces wear, and improves stability. It is used in biomedical fields [9]. Solikhov and his scientific team conducted a study investigating the effect of electrode design on high-pressure plasma xenon lamps, particularly the changes in the properties and components of the plasma [10]. A study by Timofeeva and colleagues showed that introducing thorium into arc discharge cathodes changes the illumination properties of high-pressure xenon lamps. The researchers observed that this modification significantly concentrates the emitted radiation within the visible, infrared, and ultraviolet ranges of the spectrum [11]. Mercury (Hg), a heavy metal with atomic number 80, has a relatively stable electronic structure that gives it remarkable resistance to oxidation compared to less reactive metals. This element exhibits electronic behavior similar to the noble gases, due to their similar outer energy levels. Mercury is a ubiquitous element in the environment [12]. Hg and thallium (Tl) arc lamps are used as research tools to study the nature of plasma and gas within vacuum arc discharges. These discharges are generated using innovative cathodes made of scandium deuteride, a chemical compound that combines the metallic element scandium with the heavy hydrogen isotope deuterium (which has an extra neutron). This approach contributes to a deeper understanding of the properties of both mercury and thallium within plasma environments [13,14]. This work is based on the near cathode plasma layer (NCPL) model is a theoretical physics model that simulates the ionizations and interactions occurring in the region near the cathode surface. This provides data for understanding the mechanisms of energy transfer and distribution, electron emission, and recombination, enabling improvements in the design, stability, and efficiency of arc discharge systems. The THERMCAT is a theoretical physical model that was developed to analyze current transfer mechanisms in the diffusion and spot regions, thereby contributing to electrode protection against corrosion at high temperatures and minimizing energy loss. Under specific conditions (temperature 300 K, cathode radius 0.001 mm, height 0.01 mm), mercury gas mixed with different concentrations of thallium (0.005, 0.05, 0.5 mol) was used to calculate energy flux, ratio of the ionization length to the mean free path, energy emitted from the cathode surface [15].

MODEL

The use of nonlinear surface heating to simulate current transfer to hot cathodes in high-pressure arc discharge has become an accepted and common practice [16]. The cathode plasma model is used to analyze the properties of plasma consisting of positively charged, electrons, and neutral particles [17]. The Equation 1 used to measure α – represents the ratio of the ionization length to the mean free path, $\beta = {}^{n_{i\infty}}/_{n_{a\infty}}$ represents the degree of ionization.

$$\frac{n_{a\infty}}{n_{i\infty}} = \frac{\alpha c_2\sqrt{1+\beta}}{c_2+2\alpha c_2\sqrt{1+\beta+\alpha^2}\sqrt{1+\beta}} \tag{1}$$

where: n_a is atomic number density, c_2 – dimension coefficient It is the compound density of all neutrals at the edge of the ionization layer [18].

The equations are based on the following active parameters: Schottky barrier, potential barrier, ionization energy and rate constant. The energy needed to produce a positive ion can be measured (E) [17]:

$$E = \sum_j a x_j E^{(j)} \tag{2}$$

$$k_i = \sum_l b X_l k_i^{(l)} \tag{3}$$

where: indices j and l are attributed to positive ions and to neutral species, x_j is the molar fraction of positive ions, X_l is the molar fraction of a neutral species, k_i represents the rate constant of ionization of the effective neutral particle by electron impact, $k_i^{(l)}$ is the rate constant of ionization of neutral particles of a species l by electron impact, $a = \frac{1}{\sum_j x^j}$ and $b = \frac{1}{\sum_l x^l}$ are normalization factors [19].

This Equation 4 is applied to calculate ratio of the ionization length to the mean free path (α) [20]:

$$\alpha = \sqrt{\frac{2}{3}\frac{C_{ia}Q_{ia}}{K_i}} \tag{4}$$

where: Q_{ia} is average cross section of the transmission of momentum in elastic collisions between ions and atoms. C_{ia} represents the average relative velocity between ions and atoms and is given by the Equation 5 [21]:

$$C_{ia} = \sqrt{\frac{8kT_h}{\pi}\left(\frac{1}{m_i}+\frac{1}{m_a}\right)} \tag{5}$$

$$q = q(T_w, U) \text{ where } T_w \geq T_c \tag{6}$$

$$j = j(T_w, U) \text{ where } T_w \geq T_c \tag{7}$$

where: q is the energy flux density and j is the current flux density, T_W is the temperature of cathode surface, U is the applied voltage, T_C is the temperature of center, $q(T_w, U)$ and $j(T_w, U)$ are the functions of temperature (T_w) and applied voltage (U).

When (T_w) increases, the part of the surface connected to the plasma arc heats the surface where the current is collected by the plasma, and when (T_w) decreases with the part of the surface connected to the gas this region becomes electrically isolated. (U). It represents the heat exchange of the cathode with the gas in chamber which is an air-evacuated container, it is containing mercury gas. It is used to generate plasma and confine it using a magnetic field [22].

Expression $q(T_w, U)$ is calculated by analyzing the thermal properties of the cathode material and evaluating the thermal conductivity coefficient using the approved equation.

$$\nabla.(k\nabla T) = 0 \tag{8}$$

where: $\nabla.$ is del operator, it represents derivative of a function with respect to one of its variables, k represent a thermal conductivity coefficient, ∇T is heat flow direction.

With certain limitations:

$$k\frac{\partial T}{\partial n} = q(T_w, U) \tag{9}$$

Where n represents the portion of the cathode surface that is in contact with both the arc plasma and the surrounding cold gas. This portion remains at a relatively low temperature compared to the arc plasma itself. The boundary condition for this portion is:

$$T = T_c \tag{10}$$

The cathode discharge zone model is a theoretical construct that accurately describes the behavior of plasma in the vicinity of the cathode surface during an arc discharge. This model shows that the plasma in this zone is the primary source of the energy glowing toward the surface and is also the region where the electric current is collected. This zone consists of two main components: the first is the electric charge shell directly surrounding the cathode surface, and the second is the ionization layer adjacent to this shell. The ions that arise in the ionization layer are characterized by significant acceleration under the influence of the electric field present in the vacuum charge shell (a region characterized by the absence of ion collisions), heat the interface, together with the fast electrons in the plasma, which are able to cross the work function of mercury and reach the cathode surface [22] where:

$$q_p = q_i + q_e - q_{em} \tag{11}$$

where: q_p – is the plasma energy flux density at the surface of the cathode produced. q_i – is the ions energy flux, q_e – is the electrons energy flux density, q_{em} – is the thermionic emission energy flux.

The energy flux density in Equation 1 can be written as:

$$q_i = j_i\left[\begin{matrix} ZeU + E - ZA_{eff} + \\ + k\left(2T_h + {ZT_e}/{2} - 2T_w\right)\end{matrix}\right] \tag{12}$$

$$q_e = \left(2kT_e + A_{eff}\right) \tag{13}$$

$$q_{em} = j_{em}\left(2kT_w + A_{eff}\right) \tag{14}$$

where: j_i is the current density of ions, Z is the charge state, e is the elementary charge, E is the average thermal kinetic energy of ions, A_{eff} is the effective work function, T_h is the hot ion temperature, T_e electron temperature, j_{em} is the current density of electrons emitted from the cathode surface.

Fourier's law of heat conduction was used to calculate the heat conduction energy (q) in Equation 15 [23]:

$$\mathrm{q} = -\mathrm{k}\frac{\mathrm{dT}}{\mathrm{dx}} \tag{15}$$

where: $\frac{\mathrm{dT}}{\mathrm{dx}}$ gradient of temperature.

Equation 16 used to calculate the total heat conduction energy (q_{con}), the heat flux is multiplied by the cross-sectional area:

$$q_{con} = -kA\frac{dT}{dx} \tag{16}$$

When the temperature changes linearly along the cathode:

$$q_{con} = -kA\frac{d(T_W - T_b)}{L} \tag{17}$$

where: T_b represents the base temperature, L represents the cathode length.

By adding Equations 14 and 17 Equation 18 is obtained to calculate total energy emitted from the cathode surface (Q_{em}) [23]:

$$Q_{em} = j_{em}\left(2kT_w + A_{eff}\right) - kA\frac{d(Tw-Tb)}{L} \tag{18}$$

The current density of ions (J_i) is given by Equation 1 of the Ion Flux Saturation Law [24].

$$J_i = Zen_ic_s \tag{19}$$

where: n_i represents ion number density, c_s represents the ion acoustic speed.

We use the Richardson-Dushman Equation 20 to calculate current density of emission (J_{th}).

$$J_{th} = AT_W^2 exp\left(-\frac{W}{K_BT_W}\right) \tag{20}$$

where: A represents Richardson constant, W represents work function of material, K_B represents Boltzmann constant [25].

RESULTS AND DISCUSSION

Figures 1–4 illustrates the ion energy flux (q_i), plasma energy flux (q_p), electron energy flux (q_e) and thermionic emission energy (q_{em}) of the Hg pure and when it doped with Th at concentration (0.005, 0.05, 0.5) mol at applied voltage (U= 20 V, U=50 V). In Figure 1, when the cathode surface temperature (T_W = 2000–3250 K) increases, the increase in the plasma energy glow (q_p) is large due to the rise in the electrons emitted from the cathode surface. At 20 V, the plasma energy glow is relatively stable at (T_W = 3500 K) and then begins to

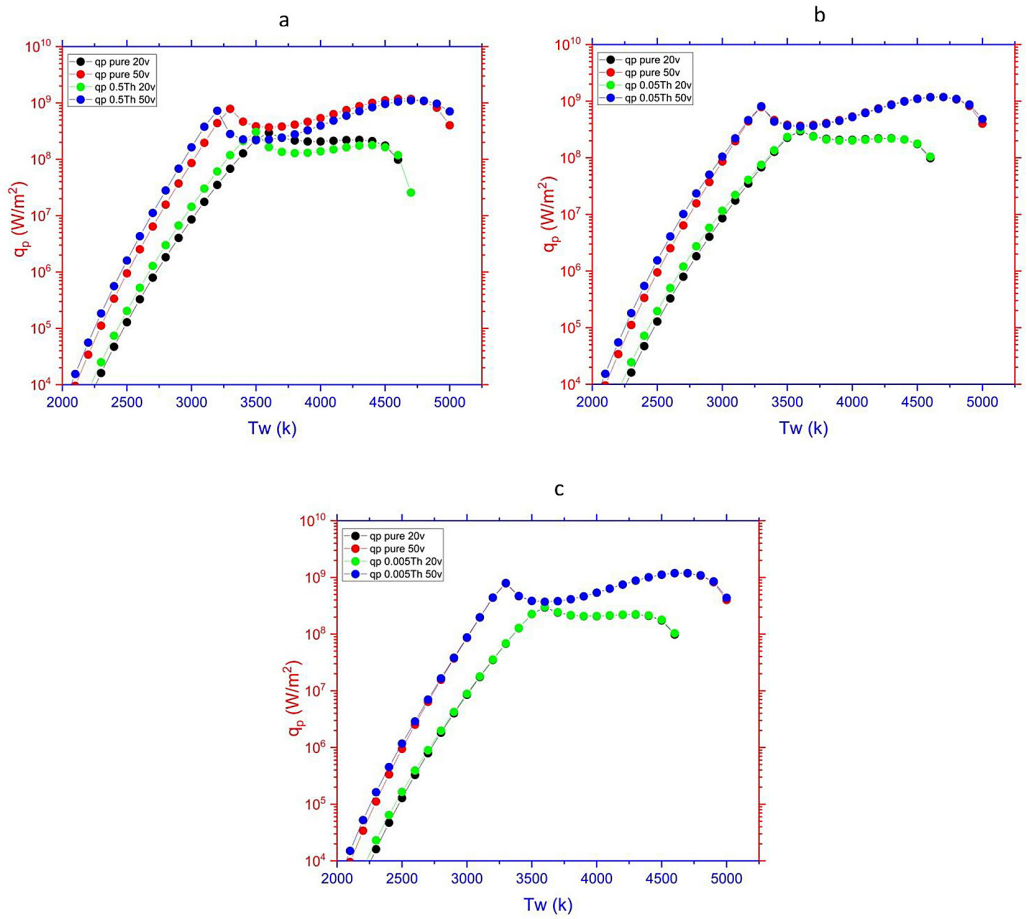

Figure 1. Plasma energy glow q_p (W/m^2) versus the cathode temperature at (a) Hg-Ti (0.5 mol), (b) Hg-Ti (0.05 mol), (c) Hg-Ti (0.005 mol)

increase slightly at high temperatures. In contrast, at a potential difference of 50 V, it is relatively stable at (T_W = 3250 K) and then begins to increase slightly at high temperatures. Figure 1a shows when adding (0.5 mol) of thallium to mercury increases the plasma energy glow by increasing the number of excited or ionized atoms (increased collisions) compared to pure mercury, where the collisions are only between electrons emitted from the cathode surface and mercury gas atoms. In turn, Figure 1b shows that when (0.05 mol) of thallium is added to mercury, there is a slight increase in the plasma energy glow of the mixture, as the increase for the mixture is at (T_W = 2000–2750 K) and at a high (T_W > 3500 K) the behavior of the mixture is similar to the behavior of pure mercury due to the weak effect of thallium. Figure 1c demonstrates that when (0.005 mol) of thallium is added to mercury, the plasma energy glow of the mixture is very close to that of pure mercury, as the effect of thallium neglects in the mixture. Increasing the applied voltage to (50 V) causes the electrons to

Table 1. Plasma energy glow q_p (W/m^2) at different concentration and applied voltage

Temperature of cathode surface T_w (K)	Hg-Ti (0.5 mol)		Hg-Ti (0.05 mol)		Hg-Ti (0.005 mol)	
	q_p (W/m^2) U=20 V	q_p (W/m^2) U=50 V	q_p (W/m^2) U=20 V	q_p (W/m^2) U=50 V	q_p (W/m^2) U=20 V	q_p (W/m^2) U=50 V
2000	559.1	3852	553.2	3824	546.3	3788
2500	203400	1598000	195900	1543000	164800	1172000
3000	1.44E7	1.63E8	1.159E7	1.049E8	8861000	8.771E7
3500	3.064E8	2.174E8	2.332E8	3.656E8	2.265E8	3.861E8
4000	1.381E8	3.964E8	2.023E8	5.22E8	2.089E8	5.387E8
4500	1.634E8	9.59E8	1.774E8	1.094E9	1.791E8	1.119E9

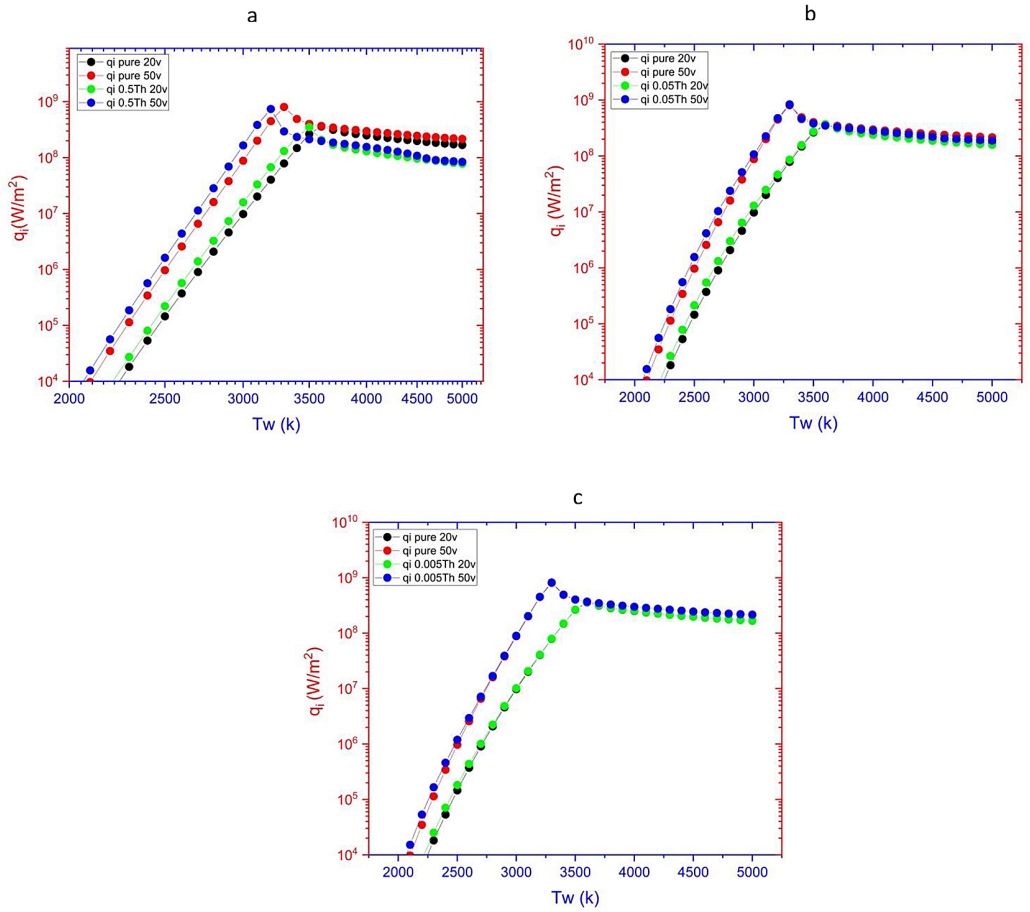

Figure 2. Ions energy flux q_i (W/m^2) versus the cathode temperature at (a= Hg-Ti (0.5 mol), b= Hg-Ti (0.05 mol), c= Hg-Ti (0.005 mol)

accelerate, which in turn raises their kinetic energy. This results in a higher number of collisions with the ions in the mixture, finally enhancing the plasma energy glow, as illustrated in Table 1. Figure 2 shows the effect of temperature (T_W) on the ions energy flux (q_i) of mixture. In Figure 2a when (0.5 mol) of thallium is added to mercury at 20 V, the ions glow energy of the mixture increases along with the temperature of the cathode surface (T_W = 2000–3500 K), and then with the increase in temperature, the ions energy flux of the mixture begins to gradually stabilize with pure mercury. At 50 V, the ions energy flux of the mixture increases along with temperature (T_W = 2000–3250 K), and then with increasing temperature, it begins to gradually stabilize with pure mercury. Figure 2b shows that when (0.05 mol) of thallium is added to mercury at 20 V, the ions energy flux of the mixture increases along with temperature (T_W = 2000–3000 K), and with increasing temperature, the behavior of the mixture is similar to that of pure mercury. At 50 V, the ion energy glow of the mixture increases along with temperature (T_W =2000–2750 K), and with increasing temperature, the behavior of the mixture is similar to that of pure mercury. Figure 2c demonstrates that when (0.005 mol) of thallium is added to mercury, the behavior of the mixture is similar to that of mercury as the temperature increases, the only effect is the potential difference on the ions energy flux of the mixture or pure mercury, as illustrated in Table 2.

The stability of the ions energy flux at high temperatures (T_W > 3500 K) is due to the high emission of electrons, which in turn works to reduce the ions energy flux and stabilize it, as the contribution of ions to energy transfer is small compared to electrons. This phenomenon is called Ion Flux Saturation [24].

Figure 3 shows the effect of temperature (T_W) on the electrons energy flux (q_e) of mixture. In Figure 3a, when (0.5 mol) of thallium is added to mercury, at 20 V, no emission of electrons energy flux occurs at low temperatures (T_W < 3550 K), the thermal threshold. When the thermal threshold is exceeded, the electrons energy flux increases rapidly and then gradually stabilizes at higher temperatures. At 50 V, electrons energy flux is emitted at (T_W > 3400 K) and increases rapidly along with temperature, and then gradually stabilizes at higher temperatures. Adding (0.5 mol) of thallium alters the thermionic emission properties, increasing electron emission and electron density. In turn, Figure 3b shows that when (0.05 mol) of thallium is added to mercury at 20 V, the emission of electrons energy flux occurs at a threshold of (T_W > 3550 K). With increasing temperature, the emission of electrons energy flux increases rapidly and then stabilizes at higher temperatures. At 50 V, the emission of electrons energy flux occurs at a threshold of (T_W > 3400 K). With increasing temperature, the emission of electrons energy flux increases rapidly and then stabilizes at higher temperatures. The addition of (0.05 mol) of thallium has a weak effect on the electron emission of the mixture. Figure 3c demonstrates that when (0.005 mol) of thallium is added to mercury, the behavior of the mixture is similar to that of pure mercury, with the effect of thallium being negligible in the mixture due to the low concentration of thallium, as illustrated in Table 3.

There is no emission of electrons energy flux for mixture or pure mercury at low temperatures, because the electrons do not have enough energy to overcome the work function. This is called sub threshold emission [26]. The stability of the electrons energy flux at high temperatures is due to reaching the saturation regime. i.e., almost all electrons are emitted [27].

Figure 4 shows the relationship between the thermionic emission energy (q_{em}) and temperature (T_W). Figure 4a shows that when (0.5 mol) of thallium is added to mercury, the thermionic emission energy increases along with temperature (T_W >

Table 2. Ions energy flux q_i (W/m^2) at different concentration and applied voltage

Temperature of cathode surface T_w (K)	Hg-Ti (0.5 mol)		Hg-Ti (0.05 mol)		Hg-Ti (0.005 mol)	
	q_i (W/m^2) U=20 V	q_i (W/m^2) U=50 V	q_i (W/m^2) U=20 V	q_i (W/m^2) U=50 V	q_i (W/m^2) U=20 V	q_i (W/m^2) U=50 V
2000	604.1	3899	598.2	3872	591.2	3835
2500	221200	1620000	213700	1564000	182200	1192000
3000	1.582E7	1.654E8	1.292E7	1.07E8	1.01E7	8.964E7
3500	3.5E8	2.126E8	2.722E8	3.814E8	2.652E8	4.045E8
4000	1.294E8	1.558E8	2.4E8	2.814E8	2.516E8	2.992E8
4500	9.63E7	1.079E8	1.879E8	2.191E8	1.992E8	2.449E8

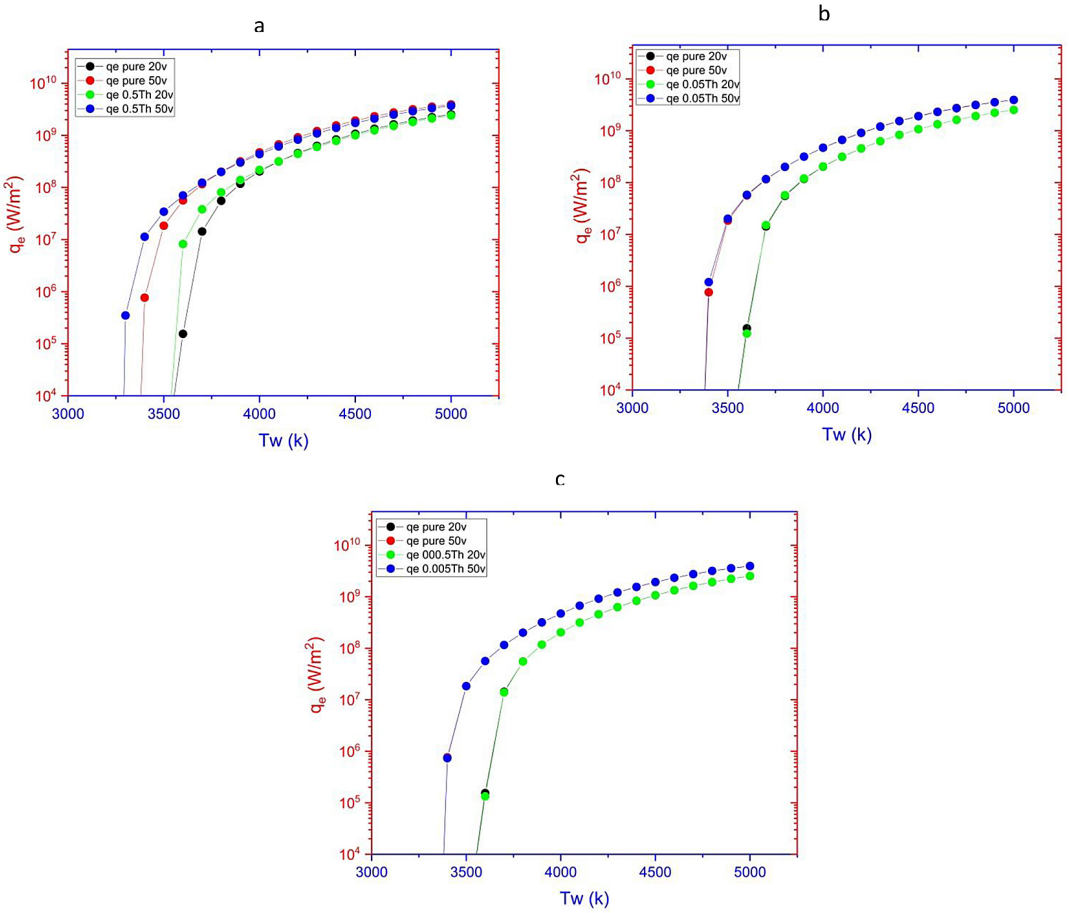

Figure 3. Electrons energy flux q_e (W/m^2) versus the cathode temperature at (a = Hg-Ti (0.5 mol), b = Hg-Ti (0.05 mol), c = Hg-Ti (0.005 mol)

Table 3. Electrons energy flux q_e (W/m^2) at different concentration and applied voltage

Temperature of cathode surface T_w (K)	Hg-Ti (0.5 mol)		Hg-Ti (0.05 mol)		Hg-Ti (0.005 mol)	
	q_e (W/m^2) U=20 V	q_e (W/m^2) U=50 V	q_e (W/m^2) U=20 V	q_e (W/m^2) U=50 V	q_e (W/m^2) U=20 V	q_e (W/m^2) U=50 V
2000	0	0	0	0	0	0
2500	0	0	0	0	0	0
3000	0	0	0	0	0	0
3500	145.3	3.428E7	317.5	2.012E7	386.4	1.838E7
4000	2.165E8	4.378E8	2.057E8	4.707E8	2.04E8	4.736E8
4500	1.005E9	1.735E9	1.072E9	1.907E9	1.077E9	1.934E9

2000 K) and is slightly greater at 50 V compared to 20 V. Adding thallium at a high concentration (0.5 mol) increases the probability of collisions due to the increased number of electrons and ions. In turn, Figure 4b presents when adding (0.05 mol) of thallium to mercury, the thermionic emission energy increases with the rise in temperature, so that the behavior of the mixture is slightly similar to the behavior of pure mercury as a result of the weak effect of thallium in the mixture. Figure 4c demonstrates that when (0.005 mol) of thallium is added to mercury, the behavior of the mixture is similar to that of pure mercury, with the effect of thallium being negligible, as illustrated in Table 4. The thermionic emission energy increases significantly along with increasing temperature according to the thermal emission equation (20) (Richardson-Dushman) as a result of increasing both the kinetic energy and the number of emitted electrons [25].

Figure 5 shows that at low temperatures (T_W < 2500 K), the a value of ratio of the ionization length to the mean free path (α) increases

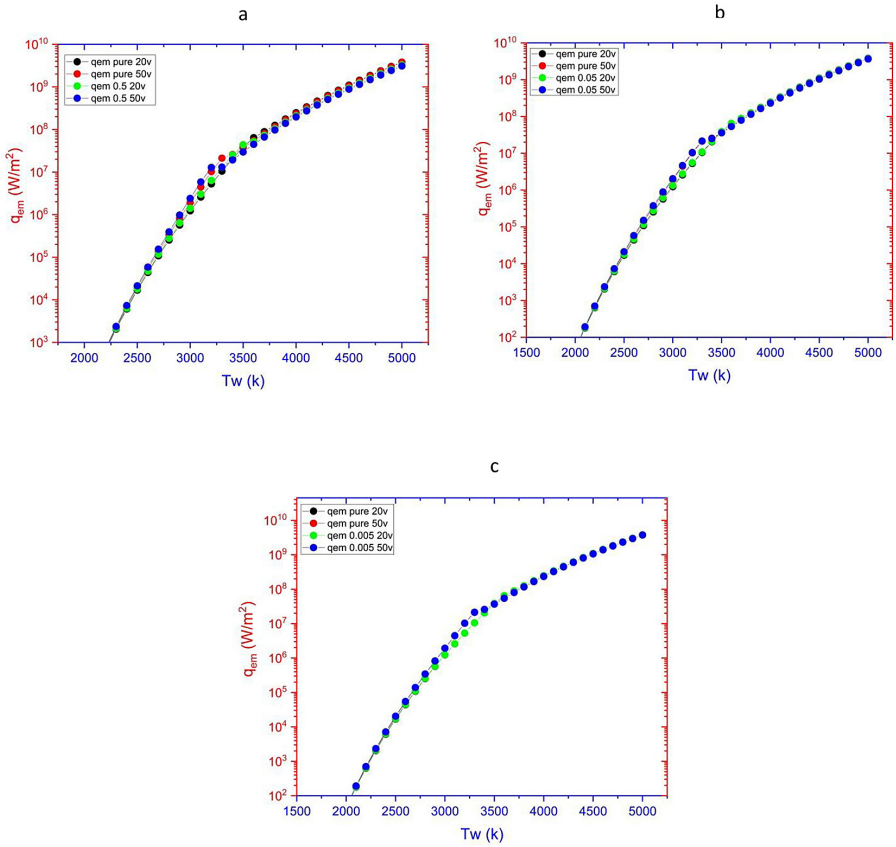

Figure 4. Thermionic emission energy q_{em}(W/m^2) versus the cathode temperature (a) Hg-Ti (0.5 mol), (b) Hg-Ti (0.05 mol), (c) Hg-Ti (0.005 mol)

Table 4. Thermionic emission energy (q_{em}(W/m^2) at different concentration and applied voltage

Temperature of cathode surface T_w (K)	Hg-Ti (0.5 mol)		Hg-Ti (0.05 mol)		Hg-Ti (0.005 mol)	
	q_{em} (W/m^2) U=20 V	q_{em} (W/m^2) U=50 V	q_{em} (W/m^2) U=20 V	q_{em} (W/m^2) U=50 V	q_{em} (W/m^2) U=20 V	q_{em} (W/m^2) U=50 V
2000	44.98	47.11	44.96	47.09	44.94	47.06
2500	17860	21300	17780	21170	17420	20320
3000	1412000	2408000	1333000	2047000	1243000	1929000
3500	4.367E7	2.949E7	3.906E7	3.597E7	3.862E7	3.677E7
4000	2.077E8	1.972E8	2.434E8	2.301E8	2.467E8	2.341E8
4500	9.378E8	8.835E8	1.082E9	1.033E9	1.097E9	1.06E9

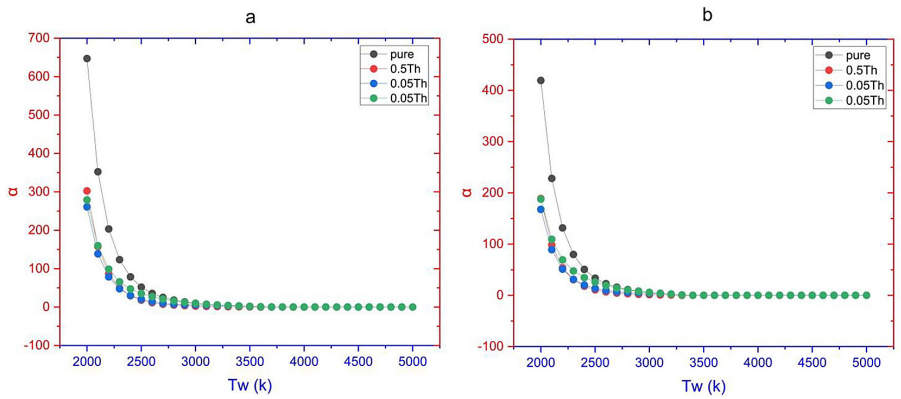

Figure 5. Ratio of the ionization length to the mean free path (α) versus the cathode temperature at (a) = 20 V, (b) = 50 V

Table 5. Ratio of the ionization length to the mean free path (α) at different concentration and applied voltage

Temperature of cathode surface T_w (K)	Hg-Ti (0.5 mol)		Hg-Ti (0.05 mol)		Hg-Ti (0.005 mol)	
	α U=20 V	α U=50 V	α U=20 V	α U=50 V	α U=20 V	α U=50 V
2000	302.5	189	260.9	167.7	279	247.1
2500	18.08	10.75	20.46	13.52	35.39	31.68
3000	2.586	1.337	5.445	4.15	9.459	5.798
3500	0.57	0.04523	1.929	0.1275	2.077	0.1498
4000	0.07023	0.03653	0.2212	0.09799	0.2579	0.1145
4500	0.05614	0.02753	0.1669	0.07849	0.1932	0.101

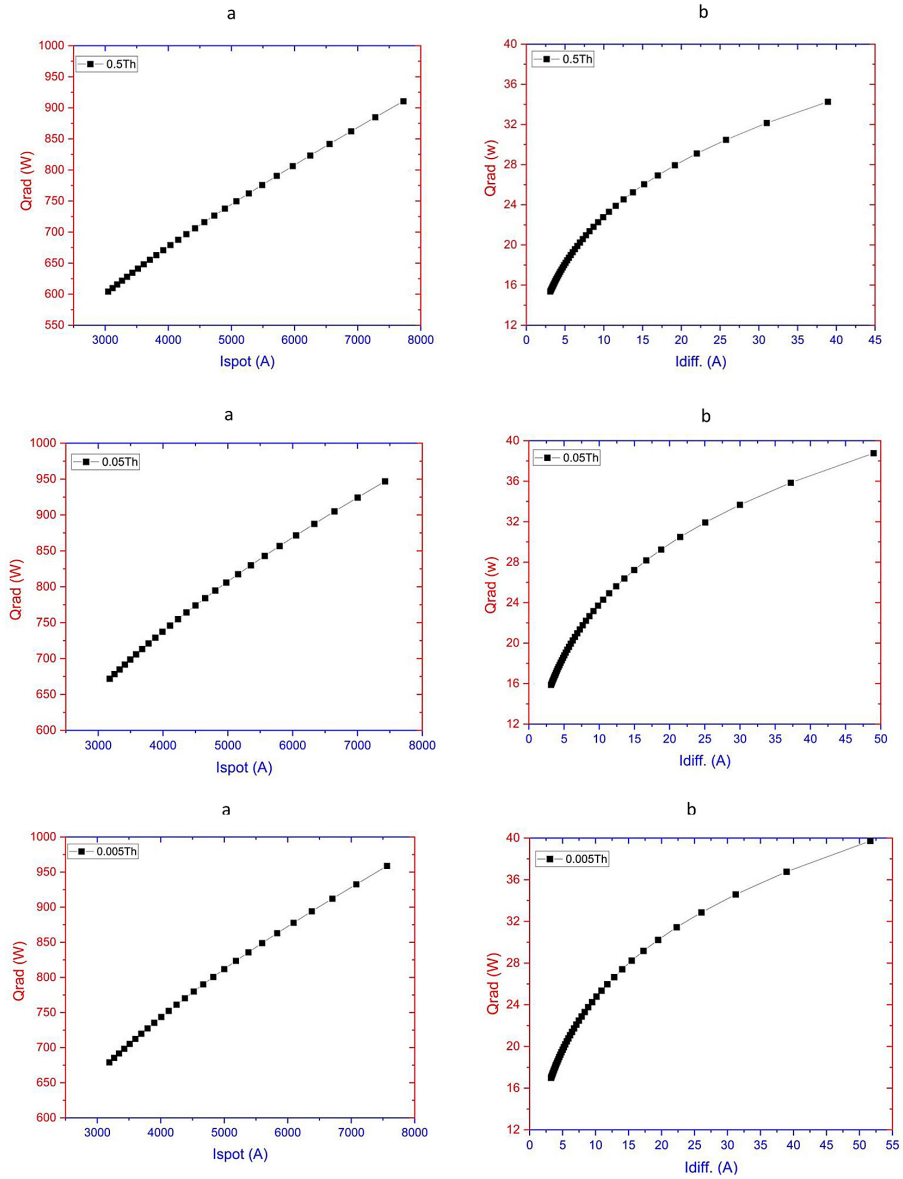

Figure 6. Energy emitted from the cathode surface Q_{rad}(W) versus at (a) = I_{spot}, (b) = $I_{diffsion}$

significantly, especially for pure mercury. However, as temperatures (T_W > 3000 K), the ratio of the ionization length to the mean free path (α) values for all concentrations converge and become close to zero. Figure 5a shows that at a low potential difference at (20 V), the effect of adding thallium to mercury is clear in reducing ratio of the ionization length to the mean free path at low temperatures.

Table 6. Energy emitted from the cathode surface Q_{rad} (W) at spot and diffusion current for different concentration of Hg-Ti mixture

No.	Hg-Ti (0.5 mol)				Hg-Ti (0.05 mol)				Hg-Ti(0.005 mol)			
	I_{spot} (A)	Q_{rad} (W)	$I_{diff.}$ (A)	Q_{rad} (W)	I_{spot} (A)	Q_{rad} (W)	$I_{diff.}$ (A)	Q_{rad} (W)	I_{spot} (A)	Q_{rad} (W)	$I_{diff.}$ (A)	Q_{rad} (W)
1	3190	615.7	3.092	15.37	3177	672	3.162	15.88	3190	679.1	3.256	17
2	3610	648.2	3.851	16.59	3584	705.9	3.958	17.23	3598	712.5	4.077	18.37
3	4156	687.7	4.875	17.99	4107	746	5.042	18.8	4125	752.3	5.195	19.94
5	4897	737.8	6.912	20.24	4806	794.8	7.24	21.36	4828	800.7	7.463	22.48
6	5971	806.2	11.53	23.9	5798	856.8	12.4	25.62	5833	863	12.81	26.66
7	7724	910.6	38.91	34.26	7425	946.9	48.97	38.77	7563	958.8	51.64	39.72

Figure 5b shows that at a high potential difference at (50 V), the addition of (0.5 mol) concentrations of thallium to mercury increases alpha at low temperatures. as illustrated in Table 5. In Figure 6, there is a relationship between the energy emitted from the cathode surface and the current. In Figure 6a, the relationship is linear between the energy emitted from the cathode surface and the spot current due to charge accumulation, making the dark area very hot. In Figure 6b, the relationship is nonlinear between the energy emitted from the cathode surface and the diffusion current, where the increase is slow due to the diffusion of electrons and charged ions. Adding thallium at a high concentration (0.5 mol) to mercury leads to an increase in the energy emitted from the cathode surface, as illustrated in Table 6.

CONCLUSIONS

In conclusion, the results clearly shows a direct relationship the between temperature (T_W) and the kinetic energy of electrons in a mercury-thallium mixture (Hg-Ti). The addition of thallium to mercury in arc discharge lamps increases the emission spectrum, resulting in an increase in the intensity of the emitted light. The addition of thallium also modifies the atomic energy levels of the mixture, resulting in improved light brightness, quality, and durability. Adding a high concentration of thallium (0.5 mol) increases the ions and electrons that contribute to light emission and durability. It also increases the efficiency of converting electrical energy into light as well as reduces energy consumption and material corrosion. The ionization potential of thallium (6.11 eV) is lower than that of mercury (10.44 eV), meaning that the energy used in the ionization process of the mixture is lower, and therefore the ionization of the mixture is quicker and easier. Increasing the applied voltage to (50 V) accelerates the charges, res ulting in ionization and collisions at lower temperatures, and there is an inverse relationship between the ratio of the ionization length to the mean free path and the cathode surface temperature, also there is a direct relationship between the spot current and the energy emitted from the cathode surface. This means that the spot current plays a significant and fundamental role in heating the cathode surface, resulting in high energy emission from the cathode electrode. In turn, the relationship between the energy emitted from the cathode surface and the diffusion current is logarithmic.

These results indicate that mercury-thallium mixture can be used in arc discharge lighting systems due to their high efficiency, and future studies can build on these results to explore the effect of other thallium concentrations.

Acknowledgements

Authors would like to thank Mustansiriyah University-Iraq, for their providing scientific service to carry out this research work.

REFERENCES

1. Sovizi S., Angizi S., Alem S.A.A., Goodarzi R., Boyuk M.R.R.T., Ghanbari H., Szoszkiewicz R., Simchi A., and Kruse P. Plasma processing and treatment of 2D transition metal dichalcogenides: tuning properties and defect engineering. Chemical reviews, 2023; 123(24): 13869–13951.
2. Cunha, M.D., M.A. Sargsyan, M.Kh Gadzhiev, D.V. Tereshonok, and M.S. Benilov. Numerical and experimental investigation of thermal regimes of thermionic cathodes of arc plasma torches. Journal of Physics D: Applied Physics, 2023; 56(39): 395204.
3. Krupski P. Design and visualization of the

ten-electrode glidarc plasma reactor using the autodesk inventor environment. Advances in Science and Technology. Research Journal, 2024; 18(7).

4. Fernando, W.T.L.S. Study on atmospheric pressure plasma jet for plasma patterning toward cell culturing, 2020.
5. Baranov O., Levchenko I., Xu S., Wang X.G., Zhou H.P., and Bazaka K. Direct current arc plasma thrusters for space applications: Basic physics, design and perspectives. Reviews of Modern Plasma Physics, 2019; 3(1): 7.
6. Millen S.L.J., and Murphy A. Modelling and analysis of simulated lightning strike tests: A review. Composite Structures, 2021; 274: 114347.
7. Saber T.A., Ali R.A., and Jawad H.M. The role of cathode heat in the Schottky correction in the ionization layers of arc plasma. Advances in Science and Technology. Research Journal, 2024; 18(4).
8. Wu Y.-S., Osman A.I., Hosny M., Elgarahy A.M., Eltaweil A.S., Rooney D.W., Chen Z. et al. The toxicity of mercury and its chemical compounds: molecular mechanisms and environmental and human health implications: a comprehensive review. Acs Omega, 2024; 9(5): 5100–5126.
9. Cejas E., Prevosto L., and Minotti F.O. Numerical simulation of the voltage–current characteristic of an atmospheric pressure discharge: the glow-to-arc transition. Plasma Chemistry and Plasma Processing, 2024; 44(2): 765–784.
10. Timofeev N. A., Solikhov D. K., Sukhomlinov V. S., and Mukharaeva I. Y. Investigation of a high-pressure short-arc xenon discharge at different electrode surface shapes with taking into account emission of cathode material into a plasma. High Energy Chemistry, 2023; 57(Suppl 1), S125–S131.
11. Timofeev N., Sukhomlinov V., Zissis G., Mukharaeva I., Borodina V., and Badr A.H. Influence of the electrode surface shape on plasma and light emission properties of high pressure short-arc xenon discharge lamps. In 2023 IEEE Sustainable Smart Lighting World Conference & Expo (LS18), 2023; 1–5.
12. Gaffney J.S., and Marley N.A. "n-depth review of atmospheric mercury: sources, transformations, and potential sinks. Energy and Emission Control Technologies, 2014; 1–21.
13. Benilov M.S. Modeling the physics of interaction of high-pressure arcs with their electrodes: advances and challenges. Journal of Physics D: Applied Physics, 2019; 53(1): 013002.
14. Korzhyk V., Strohonov D., Gao S., Tereshchenko O., Demianov O., Ganushchak O., and Wang X. Production of spherical Inconel 625 powder for additive manufacturing by plasma-arc wire atomization: Influence of non-transferred and transferred arc modes on fine powder yield. Advances in Science and Technology Research Journal, 2025; 19(11): 109–123.
15. Benilov M.S. Understanding and modelling plasma–electrode interaction in high-pressure arc discharges: a review. Journal of Physics D: Applied Physics, 2008; 41(14): 144001.
16. Yin B., Zhu Y., Chen X., and Wu Y. The capability of a deep learning based ODE solution for low temperature plasma chemistry. Physics of Plasmas, 2024; 31(6).
17. Ferreira, N.G.C., Santos D.F.N., Almeida P.G.C., Naidis G.V., and Benilov M.S. Simulation of prebreakdown discharges in high-pressure air. I: The model and its application to corona inception. Journal of Physics D: Applied Physics, 2019; 52(35): 355206.
18. Santos, D.F.N., Lisnyak M., Almeida N.A., Benilova L.G., and Benilov M.S. Numerical investigation of AC arc ignition on cold electrodes in atmospheric-pressure argon. Journal of Physics D: Applied Physics, 2021; 54(19): 195202.
19. Cunha M.D., Kaufmann H.T.C., Benilov M.S., Hartmann W., and Wenzel N. Detailed numerical simulation of cathode spots in vacuum arcs—I. IEEE Transactions on Plasma Science, 2017; 45(8): 2060–2069.
20. Martin P., Ahmed H., Doria D., Cerchez M., Hanton F., Gwynne D., Alejo A. et al. Narrow-band acceleration of gold ions to GeV energies from ultra-thin foils. Communications Physics, 2024; 7(1): 3.
21. Benilov M.S. Ionization layer with collision-free atoms at the edge of partially to fully ionized plasmas. Plasma Sources Science and Technology, 2024; 33(5): 055002.
22. Ali R.A., Hamed B., Al-obaidi M.T., and Abbas A.M. Estimation of a mathematical model for theoretical measuring of plasma electrons mobility at different concentrations of he-cu mixture. In Journal of Physics: Conference Series, 2021; 1999(1): 012132. IOP Publishing, 2021.
23. Lieberman M.A., and Lichtenberg A.J. Principles of Plasma Discharges and Materials Processing. John Wiley & Sons, 2024.
24. Pekker L. A sheath collision model with thermionic electron emission and the Schottky correction factor for work function of wall material. Plasma Chemistry and Plasma Processing, 2017; 37(3): 825–840.
25. De D.K., and Olawole O.C. Modified Richardson-Dushman equation and modeling thermionic emission from monolayer graphene. In: Nanoengineering: Fabrication, Properties, Optics, and Devices 2016; XIII, 9927: 59–65. SPIE.
26. Luo H., et al. On the Origin of Sub-Threshold Turn-On in Quantum-Dot Light-Emitting Diodes. ACS Nano, 2019; 13(7).
27. Smith J.R., et al. Theory of space charge limited regime of thermionic energy converter with negative electron affinity emitter. Journal of Vacuum Science & Technology B: Microelectronics and Nanometer Structures Processing, Measurement, and Phenomena, 2009; 27(3): 1132.